Staphylococcus aureus Fibronectin-Binding Protein Serves as a Substrate for Coagulation Factor XIIIa: Evidence for Factor XIIIa-Catalyzed Covalent Cross-Linking to Fibronectin and Fibrin

Yury V. Matsuka,*,‡ Elizabeth T. Anderson,‡ Tammy Milner-Fish,‡ Peggy Ooi,§ and Steven Baker||

Department of Protein Chemistry, Biotechnology Group, and Department of Bacteriology, Wyeth Research, Pearl River, New York 10965

Received July 15, 2003; Revised Manuscript Received September 17, 2003

ABSTRACT: In this study, we have investigated the interactions of a Staphylococcal recombinant fibronectin-binding protein A (rFnbA) with fibronectin, fibrinogen, and fibrin. Using analytical size-exclusion chromatography, we evaluated the stoichiometry of reversible binding of FnbA to fibronectin and demonstrated that, in solution, it can accommodate at least two molecules of fibronectin. Results of ELISA experiments demonstrated that rFnbA binds with equally high affinity to both immobilized fibrinogen and fibrin. When included into a thrombin-induced fibrin polymerization reaction, rFnbA strongly inhibited fibrin assembly in a dose-dependent manner. In this study, we have shown that rFnbA can act as a substrate for coagulation factor XIIIa. Factor XIIIa catalyzes the incorporation of amine donor (dansylacadaverine) and amine acceptor (peptide patterned on the N-terminal sequence of fibronectin) synthetic probes into rFnbA, suggesting that it serves as a bifunctional substrate containing reactive glutamine and lysine residues. We have demonstrated that the reversible complex formed by rFnbA and fibronectin or rFnbA and fibrin is covalently stabilized by the transglutaminase action of factor XIIIa. Incubation of rFnbA in the presence of either of its ligands and factor XIIIa results in the introduction of intermolecular ϵ-(γ-glutamyl)lysine isopeptide bond(s) and the formation of high molecular mass heteropolymers. These findings suggest a novel mechanism by which pathogenic *Staphylococcus aureus* may utilize the transglutaminase activity of factor XIIIa for attachment to soluble proteins, cell surfaces, and matrixes.

The ability of pathogenic *Staphylococcus aureus* to recognize and bind human extracellular matrix (ECM) proteins is one of its most prominent features. Adherence of *S. aureus* to host tissues is believed to be a critical step in colonization and subsequent establishment of infection. *S. aureus* cells express several surface-associated proteins that specifically recognize various ECM components including fibronectin and fibrin(ogen) (*1*). Staphylococcal surface-associated fibronectin-binding protein (M_r = 110 kDa) is a single polypeptide chain receptor responsible for the binding of the bacteria to both fibronectin (*2*, *3*) and fibrinogen (*4*). Fibronectin-binding protein from *S. aureus* belongs to the family of MSCRAMM receptors (microbial surface components recognizing adhesive matrix molecules) and shares common structural−functional properties with fibronectin receptors from other Gram-positive bacteria (*1*, *5*). Most *S. aureus* strains express one (FnbA) or two (FnbA and FnbB) homologous fibronectin-binding proteins encoded by two linked genes (*6*, *7*). The NH_2-terminal region of the mature staphylococcal fibronectin-binding protein is formed by an extended, ∼500 residues long sequence A that is interrupted within FnbA by two copies of a ∼30-residues long sequence

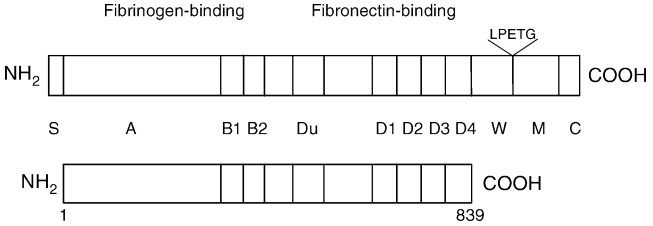

FIGURE 1: Schematic illustration of the structural organization of FnbA from *S. aureus* strain ATCC49525 (top) and recombinant FnbA (residues Ala1−Pro839) used in this study (bottom). The cartoon shows the location of the major regions: S−NH_2-terminal signal sequence; A−fibrinogen-binding region; B1 and B2−homologous repeats of unknown function; Du, D1, D2, D3, and D4−fibronectin-binding repeats; W−wall-spanning region; M−membrane-spanning region; and C−COOH-terminal cytoplasmic segment. Also shown is the position of the LPETG motif involved in the anchoring of FnbA to the cell wall peptidoglycan.

B (Figure 1). The double copy of the B sequence is missing in the FnbB version of the protein. The NH_2-terminal A region of fibronectin-binding protein forms a fibrinogen-binding site similar to that of Staphylococcal clumping factor (*4*). The fibronectin-binding site is localized within the COOH-terminal region of the protein and is composed of three full copies (37−40 residues, D1-3) and one partial copy (19 residues, D4) of the D1-4 repeat. A fifth, Du repeat is separated from the D1-4 segment by a 100 residues long insert and is adjacent to the NH_2-terminal A region (*6*−*8*). The COOH-terminal extension of the fibronectin-binding

* Address correspondence to the following author. Telephone: (845) 602-8366. Fax: (845) 602-4350. E-mail: matsukay@wyeth.com.
‡ Department of Protein Chemistry.
§ Biotechnology Group.
|| Department of Bacteriology.

10.1021/bi035239h CCC: $25.00
Published on Web 11/18/2003

protein is organized similarly to that of other surface-associated proteins from Gram-positive bacteria and composed of cell wall repeats W, an LPETG cell wall anchoring motif, membrane-spanning region M, and the cytoplasmic segment C (*1*, *9*).

Both fibrinogen and fibronectin are multifunctional adhesive proteins that play a major role in many important physiological processes, such as thrombosis, haemostasis, and wound healing (*10*, *11*). Thrombin-mediated conversion of fibrinogen to fibrin results in spontaneous polymerization of the latter and the formation of a clot that prevents the loss of blood upon vascular injury, as well as serving as a provisional matrix in subsequent tissue repair. During the late stage of the blood coagulation process, the fibrin polymer is stabilized by the transglutaminase action of factor XIII. Thrombin-activated plasma transglutaminase, or factor XIIIa, catalyzes covalent cross-linking in the γ- and α chains to produce cross-linked fibrin with increased mechanical stability (*10*, *12*). Fibrin polymerization is also accompanied by the incorporation of fibronectin into the clot (*13*). This reaction occurs in two stages. First, fibronectin binds reversibly to fibrin and then becomes covalently cross-linked to it by factor XIIIa (*14*−*17*). The presence of fibronectin in the clot matrix is important to the cell adhesion and migration events required for the wound healing process (*18*−*20*). Factor XIIIa catalyzes fibrin/fibrin and fibrin/fibronectin cross-linking through the formation of intermolecular ϵ-(γ-glutamyl)lysine isopeptide bonds between a reactive glutamine and the ϵ-amino group of a reactive lysine residues. Cross-linking occurs via an acyl transfer reaction in which the γ carboxyamide group of glutamine serves as the acyl-donor (amine-acceptor), and the ϵ-amino group of lysine serves as the acyl-acceptor (amine-donor) (*12*, *21*). The substrate specificity of plasma transglutaminase is extremely stringent, and only a limited number of proteins undergo this cross-linking reaction. Such proteins specifically associate with each other to form a reversible (noncovalent) complex and only then become covalently cross-linked by factor XIIIa. Thus, the fact that the two main physiological substrates for factor XIIIa (i.e., fibronectin and fibrin(ogen)) both interact with the Staphylococcal surface-associated receptor raises the possibility that the fibronectin-binding protein might undergo factor XIIIa-catalyzed cross-linking to its ligands. To address this issue, we have investigated the reversible interaction and factor XIIIa-catalyzed covalent cross-linking of the fibronectin-binding protein with fibronectin and fibrin(ogen). We have shown that the Staphylococcal fibronectin-binding protein serves as a substrate for factor XIIIa and undergoes covalent cross-linking to human fibronectin and fibrin, resulting in the formation of heteropolymers. These findings suggest a novel mechanism by which pathogenic *S. aureus* may attach to plasma proteins, cell surfaces, and extracellular matrixes.

EXPERIMENTAL PROCEDURES

Expression and Purification of Recombinant Fibronectin-Binding Protein A (rFnbA). The region of the *fnb*A gene encoding fibronectin binding protein A amino acid residues 1−839 (Figure 1) was produced by PCR amplification using chromosomal DNA from *S. aureus* strain ATCC49525 as template. To clone the *fnb*A gene, we designed the following forward 5′-GGCCATGGCATCAGAACAAAAGACAACTACAG-3′ and reverse 5′-CGAGGATCC*TT*ACGGCGTTGTATCTTCTTCAATCG-3′ PCR primers. The forward primer incorporated an *Nco*I restriction site (underlined) and ATG initiation codon immediately before the coding region of the mature sequence. The reverse primer included a TAA stop codon immediately after the coding segment, followed by a *Bam*HI site (underlined). The amplified DNA fragment was purified by electrophoresis in agarose gel, sequentially digested with *Nco*I and *Bam*HI restriction enzymes, and ligated into the pET-28a expression vector (Novagen, Inc.). The resulting plasmid was used for transformation of TOP10 and then BL21(DE3)pLysS *E. coli* host cells. The cloned DNA fragment of the *fnb*A gene was sequenced to confirm the integrity of the entire coding region. For expression of the FnbA, BL21 cells were grown at 37 °C in Luria broth medium containing 30 μg/mL kanamycin and 30 μg/mL chloramphenicol. Overnight cultures were diluted 1:100 with fresh Luria broth medium, grown for 2 h at 37 °C (mid-log phase), induced with 0.4 mM isopropyl-1-thio-β-D-galactopyranoside for 2−3 h, harvested by centrifugation, and lysed by the freeze−thaw method. The soluble fraction of the bacterial lysate was isolated from cell debris by centrifugation and then sequentially fractionated with 25 and 40% (w/v) of ammonium sulfate. The material precipitated with 40% ammonium sulfate was collected by centrifugation, dissolved in 20 mM Tris, pH 7.4, 1 M NaCl, 2 M urea, and applied to a Superose-6 size-exclusion column (Amersham Pharmacia Biotech) equilibrated with the same buffer. Fractions containing rFnbA were pooled, dialyzed against 20 mM Tris, pH 7.4, 25 mM NaCl, and applied to a Fractogel TMAE anion exchange column (EM Separations), equilibrated with the same 20 mM Tris, pH 7.4, 25 mM NaCl buffer. Material bound to the anion-exchange resin was eluted with a 0−75% linear gradient of NaCl using 20 mM Tris, pH 7.4, 1 M NaCl buffer. Fractions containing rFnbA were collected, pooled, and dialyzed against 20 mM Tris, pH 7.4, 150 mM NaCl. Purified rFnbA samples were aliquoted and stored frozen at −20 °C. The identity of isolated rFnbA was confirmed using SDS−PAGE and NH_2-terminal sequence analysis. Purified rFnbA exhibited a single band on SDS−PAGE and displayed a single NH_2-terminal sequence starting at *M*ASEQKTTTVE.

Preparation of Fluorescein Isothiocyanate Labeled rFnbA. Recombinant FnbA was labeled with fluorescein isothiocyanate (FITC) by incubating 1 mg of protein with a 5-fold molar excess of FITC on Celite (Sigma) in 1 mL of 0.1 M $NaHCO_3$ buffer, pH 9.5, for 2 h at 37 °C. Excess of FITC/Celite was removed by centrifugation, and the supernatant was applied to PD-10 column (Amersham Pharmacia Biotech) and equilibrated with TBS, pH 7.4 buffer. Absorbance at 280 and 495 nm was monitored. Fractions of FITC labeled rFnbA were pooled, and the degree of labeling was estimated optically (*22*) to be about 2 mol of dye/mol of protein.

Analytical Size-Exclusion Chromatography Experiments. These measurements were performed at room temperature on a Superose-6 10/30 column (Amersham Pharmacia Biotech) using a Dynamax HPLC station equipped with a ProStar fluorescence detector (Varian). Samples of FITC-rFnbA mixed with various amounts of human fibronectin (Sigma) in TBS, pH 7.4 were applied to the column at a flow rate of 0.3 mL/min, while monitoring elution by fluorescence at 525 nm with excitation at 495 nm. Concentration of the FITC-rFnbA was always 0.214 μM, while

concentration of the fibronectin varied from 0 to 0.428 μM. The volume of the sample loaded on the column was 0.25 mL in all experiments. Analysis of elution profiles was performed using the Rainin Dynamax data reprocessing program available with the Dynamax HPLC station.

Antibodies. Anti-rFnbA polyclonal antibodies were generated by intradermal immunization of female New Zealand White rabbits with 50 μg of rFnbA in the presence of complete Freund's adjuvant at week 0, followed by subsequent intramuscular immunizations with 100 μg of protein in the presence of incomplete Freund's adjuvant at weeks 4 and 8. Samples of rabbit sera were collected at weeks 0 (before the first immunization), 6, and 10. Antiserum collected at week 10 was used in this study. The mouse monoclonal anti-FITC antibody (clone FL-D6) alkaline phosphatase conjugate was purchased from Sigma. Mouse monoclonal anti-fibronectin antibody (clone Z055) was purchased from Zymed Laboratories Inc. Mouse monoclonal anti-fibrinogen Aα chain (Aα 529−539, clone 1C2-2) and anti-fibrinogen γ chain (γ 95−265, clone 44-3) antibodies were obtained from Accurate Chemical and Scientific Corp. Goat anti-rabbit and anti-mouse IgG alkaline phosphatase or horseradish peroxidase conjugates were purchased from BioRad Laboratories.

SDS−PAGE and Western Blot Analysis. SDS−PAGE was carried out using precast 4−20% (BioRad Laboratories) or 3−8% (Invitrogen) gradient gels. All SDS−polyacrylamide gels in this study were stained with Coomassie Brilliant Blue R (BioRad Laboratories). For Western Blot analysis, protein samples were electroblotted to nitrocellulose membranes and immunostained with the corresponding rabbit polyclonal or mouse monoclonal antibody. The membranes were treated with goat anti-rabbit or anti-mouse alkaline phosphatase-conjugated secondary antibody, and alkaline phosphatase activity was developed with alkaline phosphatase conjugate substrate (BioRad Laboratories).

Solid-Phase Binding Assay. Solid-phase binding was performed in plastic microtiter plates (Nunc) using an enzyme-linked immunosorbent assay (ELISA). Microtiter plate wells were coated overnight at 4 °C with 100 μL/well of 3 μg/mL fibronectin (Sigma), fibrinogen (Calbiochem), and BSA (Sigma) in 100 mM Na_2CO_3, pH 9.5 or TBS, pH 7.4 buffer. To convert fibrinogen into fibrin, wells with adsorbed fibrinogen were treated with 100 μL/well of thrombin (1 NIH U/mL) at 37 °C for 1 h in TBS, 5 mM $CaCl_2$, pH 7.4. The wells were then blocked with 5% nonfat milk in TBS for 1 h at 37 °C. After washing with TBS containing 0.05% Tween-20 (TBS-Tween), the indicated concentrations of rFnbA or FITC-rFnbA species were added to the wells in TBS, pH 7.4 buffer and incubated for 2 h at 37 °C. Bound rFnbA was detected with rabbit polyclonal antibody to rFnbA, followed by goat anti-rabbit IgG horseradish peroxidase conjugate. Peroxidase activity was developed using ABTS Microwell Peroxidase Substrate (Kirkegaard and Perry Laboratories Inc.). Bound FITC-rFnbA was detected with mouse monoclonal anti-FITC antibody alkaline phosphatase conjugate. Phosphatase activity was developed using Alkaline Phosphatase pNPP Substrate (Sigma). Bound rFnbA and FITC-rFnbA species were measured spectrophotometrically at 405 nm. The data were fitted by nonlinear regression analysis using eq 1:

$$A = A_{max}[L]/K_d + [L] \quad (1)$$

where A represents the amount of ligand bound, A_{max} is the amount of ligand bound at saturation, [L] is the molar concentration of free ligand, and K_d is the dissociation constant.

Fibrin Polymerization Turbidity Measurements. Polymerization of fibrin was measured as an increase of turbidity (light scattering) at 350 nm as a function of time using a Spectronic Genesis 2 spectrophotometer (Spectronic Instruments, Inc.), equipped with a thermostatic cell holder or Spectra Max Plus 384 microplate reader (Molecular Devices). Polymerization reactions were performed either in 10 mm path cells or in microtiter plate wells, respectively. Fibrin polymerization was initiated by the addition of 0.1−0.05 U/mL thrombin (Sigma) to 1 μM fibrinogen (Calbiochem) in TBS, pH 7.4 buffer containing 5 mM $CaCl_2$. Low concentrations of thrombin were used so that all three phases of clotting, lag phase, turbidity rise, and final turbidity could be monitored. The effect of rFnbA on fibrin assembly was evaluated by incorporating increasing concentrations of rFnbA into the reaction mixture prior to the addition of thrombin. BSA and Fn were utilized in control reactions. All fibrin polymerization experiments were performed at 25 °C.

Factor XIIIa Catalyzed Cross-Linking Reactions. Cross-linking with fibronectin was initiated by addition of 0.25 U/mL thrombin (Sigma) to a solution containing 2 μM rFnbA, 1 μM human fibronectin (Sigma), and 15 μg/mL human factor XIII (Haematologic Technologies, Inc.). The reactions were carried out in TBS, pH 7.4 buffer containing 5 mM $CaCl_2$ at 25 °C. At various times thereafter, cross-linking reactions were terminated by the addition of 2% SDS and 10% β-mercaptoethanol, heated at 95 °C, and analyzed by SDS−PAGE/Western blotting. Factor XIIIa-catalyzed cross-linking of fibrin in the presence or absence of 2 μM rFnbA was initiated by the addition of 0.5 U/mL thrombin to a solution containing 5 μM human fibrinogen and 15 μg/mL factor XIII. Cross-linking reactions were terminated at various times by the addition of 20 mM Tris, pH 7.2, 9 M urea, 40 mM dithiothreitol, 2% SDS (*23*). The clots were solubilized at 37 °C for 30 min, and heated at 95 °C, and samples were analyzed by SDS−PAGE/Western blotting. Preactivated factor XIII was used to incorporate dansylcadaverine (Sigma) or dansyl-ϵ-aminocaproyl-QQIV (custom synthesized by New England Peptide, Inc.) into rFnbA. For this purpose, 500 μg/mL factor XIII was activated by treatment with 0.25 U/mL thrombin in TBS, pH 7.4 buffer containing 10 mM dithiothreitol and 20 mM $CaCl_2$. After incubation for 20 min at 37 °C, thrombin was inactivated by the addition of hirudin (Sigma), and this mixture was used as factor XIIIa. Dansylcadaverine was used to probe factor XIIIa-reactive glutamines, and the peptide dansyl-ϵ-aminocaproyl-QQIV was used to probe reactive lysines (*24*, *25*). Incorporation was carried out by incubating 2 μM rFnbA with 30 μg/mL factor XIIIa in the presence of either 2 mM dansylcadaverine or 2 mM dansyl-ϵ-aminocaproyl-QQIV in TBS, pH 7.4, 5 mM dithiothreitol, 5 mM $CaCl_2$ at 37 °C. At various times, reactions were terminated by the addition of 2% SDS and 10% β-mercaptoethanol, heated at 95 °C, and analyzed by SDS−PAGE. Gels were examined under

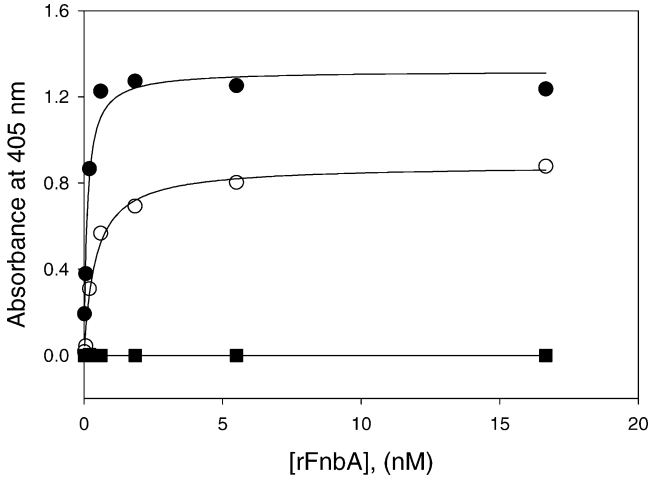

FIGURE 2: Binding of rFnbA to immobilized fibronectin as determined by ELISA. Increasing concentrations of rFnbA (●) or FITC-rFnbA (○) were incubated in microtiter wells coated with fibronectin or BSA (■) as a control. Bound rFnbA species were detected with polyclonal anti-rFnbA or monoclonal anti-FITC antibody. The data are representative of four experiments, each performed in duplicate. Curves represent the best fit of the data to eq 1. The K_d for interaction of rFnbA- and FITC-labeled rFnbA with fibronectin was found to be 0.12 ± 0.04 and 0.79 ± 0.3 nM, respectively.

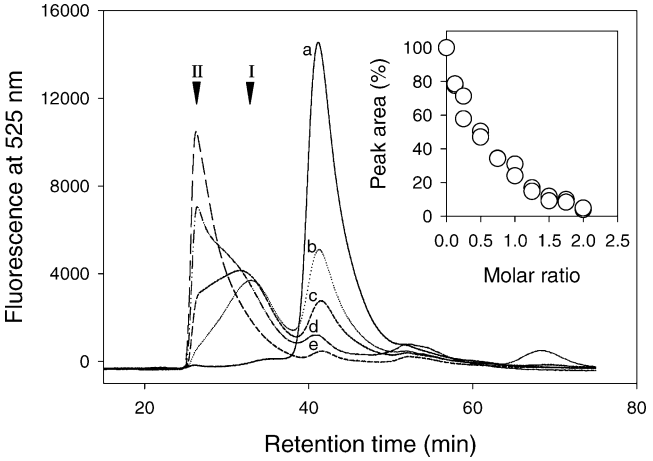

FIGURE 3: Interaction of rFnbA with fibronectin as determined by analytical size-exclusion chromatography on Superose-6. Size-exclusion chromatography elution profile of the FITC-labeled rFnbA alone (a) and FITC-rFnbA mixed with 0.5 (b), 1.0 (c), 1.5 (d), and 2 (e) molar equivalents of fibronectin are shown. Peaks corresponding to the heterocomplex formed at different molar ratios of FITC-rFnbA to fibronectin are labeled by arrows and depicted as I and II. The inset shows the decrease in area of the FITC-rFnbA peak plotted vs the molar ratio of FITC-rFnbA to fibronectin. The amount of FITC-rFnbA applied was constant in all cases. At each molar ratio, two size-exclusion chromatography runs were performed, and the data from all experiments was included in the graph.

ultraviolet light and then stained with Coomassie Brilliant Blue.

RESULTS

Reversible Interaction of Fibronectin-Binding Protein with Fibronectin. Interaction of recombinant fibronectin-binding protein (residues Ala1 to Pro839) with fibronectin was evaluated by two methods: ELISA and analytical size-exclusion chromatography. In ELISA-based assays, both fibronectin-binding protein and its fluorescein-labeled derivative specifically interacted with the immobilized fibronectin in a dose-dependent manner (Figure 2). Detection of bound rFnbA and FITC-rFnbA was performed with polyclonal anti-rFnbA and monoclonal anti-FITC antibody, respectively. The solid lines on ELISA graphs represent the best fits of the experimental data to eq 1 yielding dissociation constants of 0.12 nM for fibronectin-binding protein and 0.79 nM for fluorescein-labeled fibronectin-binding protein. Thus, the ELISA data confirmed functional (binding) activity of rFnbA Ala1 to Pro834 and indicated that fluorescein labeled rFnbA still exhibits strong affinity toward fibronectin. Binding of rFnbA to fibronectin was further investigated using analytical size-exclusion chromatography. Since the affinity of Staphylococcal fibronectin-binding protein to human fibronectin is extremely high (K_d = 0.12−0.79 nM), it is possible to estimate the stoichiometry of the complex by application of the well-defined mixtures of both proteins to the size-exclusion column, monitoring the decrease of the peak area corresponding to the one protein component and the increase of the complex. However, when applied to Superose-6 column, both fibronectin-binding protein and fibronectin eluted with very similar retention times of 40.46 and 40.00 min (not shown), making it impossible to distinguish between peaks corresponding to individual protein components. To resolve this problem, we utilized the fluorescein-labeled fibronectin-binding protein and detected its elution from the column by monitoring fluorescence intensity at 525 nm with excitation at 495 nm. As shown in Figure 3, increasing the proportion of fibronectin in the mixture caused the decrease of fluorescence intensity of the peak corresponding to FITC-rFnbA and the appearance of a new fluorescence peak I corresponding to a heterocomplex. Further increase of the fibronectin proportion in the mixture resulted in a continuous decrease of the intensity of the peak corresponding to FITC-rFnbA, which was accompanied by evolution of the heterocomplex peak I. The latter became broader and eventually transformed into a new heterocomplex peak II eluting ahead of both complex I and fibronectin-binding protein alone (Figure 3). In the presence of a two molar excess of fibronectin in the mixture, the peak corresponding to free FITC-rFnbA completely disappeared. A plot of the peak area of the fluorescein-labeled fibronectin-binding protein versus the molar ratio in the mixture reveals that Staphylococcal rFnbA does bind at least two molecules of plasma fibronectin (Figure 3, inset). Since the amount of free FITC-rFnbA is already exhausted in the presence of two molar excess of fibronectin, further increase the proportion of fibronectin in the mixture cannot be utilized for the evaluation of possible formation of higher order complexes. Detection of such complexes eluting from the column in front of complex II is also restricted by column void volume. Thus, these data suggest that, in solution, FnbA can accommodate two or more molecules of fibronectin.

Reversible Interaction of Fibronectin-Binding Protein with Fibrinogen and Fibrin. Binding of fibronectin-binding protein to fibrinogen and fibrin was investigated using ELISA and the fibrin polymerization assay. In ELISA experiments, to make absorption of fibrinogen and fibrin to microplate wells more uniform, all wells were first coated with fibrinogen, and then some of them were treated with thrombin to convert fibrinogen into fibrin (see Experimental Procedures). Figure 4 presents typical examples of ELISA-based binding experiments of fibronectin-binding protein

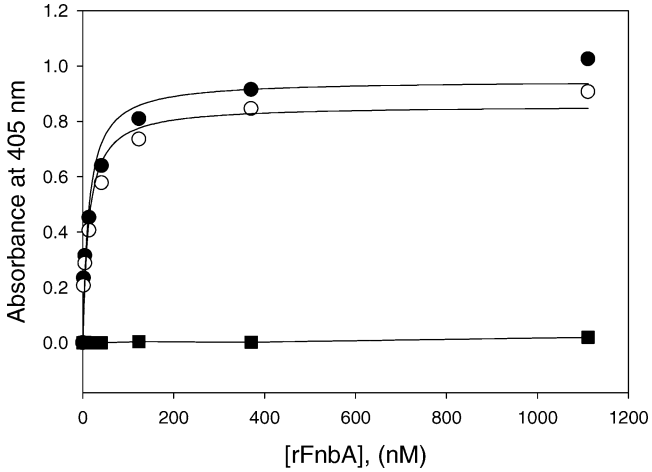

FIGURE 4: Binding of rFnbA to immobilized fibrinogen and fibrin as determined by ELISA. Increasing concentrations of rFnbA were incubated in microtiter wells coated with fibrinogen (○), fibrin (●), or BSA (■) as a control. Bound rFnbA species were detected with polyclonal anti-rFnbA antibody. The data are representative of four experiments, each performed in duplicate. Curves represent the best fit of the data to eq 1. The K_d for interaction of rFnbA with fibrinogen and fibrin was found to be 30.2 ± 4 and 29.3 ± 6 nM, respectively.

with fibrinogen and fibrin. Fibronectin-binding protein binds equally well to fibrinogen and fibrin coated plates. In both cases, titration resulted in a dose-dependent binding curve with a well-defined saturation plateau. Determination of dissociation constants for fibrinogen and fibrin resulted in values of 30.2 and 29.3 nM, respectively (Figure 4). To further characterize the interaction between the two proteins and to gain understanding of how the fibronectin-binding protein might influence the functional properties of fibrin(ogen), we examined the effect of rFnbA on the thrombin-catalyzed fibrin polymerization reaction. Light scattering measurements were used to monitor the effects of fibronectin-binding protein on fibrin assembly (*26*). Measurements of light scattering (turbidity) over the time of fibrin clot formation allow monitoring of different stages of polymerization (*26*, *27*). In the initial lag phase, monomeric fibrin forms long two-stranded protofibrils, which do not affect light scattering. In a second phase, fiber growth occurs by lateral association and branching of protofibrils, which is accompanied by a rapid rise of turbidity. In a third plateau phase, fibrin assembly (network of fibrin fibers) is nearly completed; therefore, turbidity either stabilizes or continues to increase slowly (Figure 5A, upper curve). The influence of rFnbA on the assembly of clot was examined by addition of increasing concentrations of rFnbA to fibrinogen prior to thrombin-induced polymerization. As shown in Figure 5A, fibrin polymerization was drastically affected by the presence of fibronectin-binding protein. Within the 0.02−0.2 μM concentration range of rFnbA, there was a striking decrease in the rate of turbidity rise and maximum turbidity and an increase in the lag period (Figure 5A). In the presence of 0.5 μM rFnbA, the fibrin polymerization process was entirely inhibited. Maximum turbidity values plotted as a function of different molar concentrations of rFnbA added into the reaction mixture indicate that inhibition of fibrin assembly occurs in a dose-dependent manner (Figure 5B). Inhibitory activity of rFnbA reaches its maximum at a molar ratio of rFnbA/fibrin of 1:2. Bovine serum albumin and human

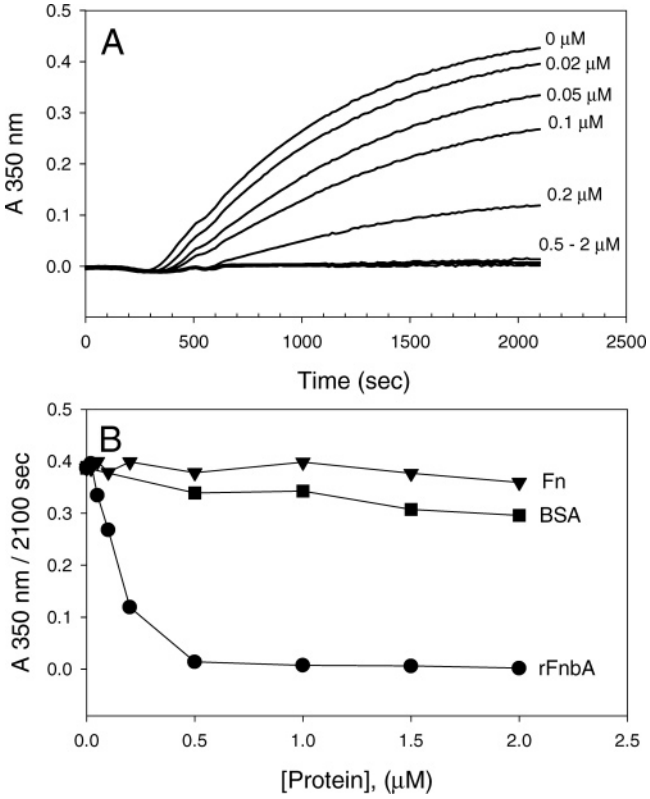

FIGURE 5: Effect of rFnbA on fibrin polymerization. Panel A, fibrin polymerization in the absence (upper curve) and presence of the indicated concentrations of rFnbA. Polymerization was initiated by the addition of thrombin (0.05 U/mL) at time zero to 1 μM fibrinogen, and polymer formation was measured as a change in turbidity at 350 nm with time. Panel B, changes in turbidity after 35 min has been plotted as a function of different concentrations of rFnbA (●) or Fn (▼) and BSA (■) as a control. There is a sharp dose-dependent decrease in turbidity with added rFnbA up to 0.5 μM, at which the inhibitory effect reaches its maximum, and fibrin polymerization is completely blocked.

fibronectin, tested in control reactions, had no effect on fibrin polymerization (Figure 5B). The previous data indicate that Staphylococcal rFnbA inhibits the fibrin polymerization reaction by affecting all three phases of fibrin assembly.

Fibronectin-Binding Protein Is a Target for Cross-Linking by Factor XIIIa. It is well-established that tissue or plasma transglutaminases incorporate specific amine-donor and -acceptor synthetic probes into their protein substrates (*21*, *23*, *25*). To examine the possibility that the fibronectin receptor from *S. aureus* serves as a substrate for activated coagulation factor XIII (factor XIIIa), we asked if it could incorporate the fluorescent amine-donor synthetic probe dansylcadaverine and amine-acceptor dansyl-ϵ-aminocaproyl-QQIV peptide. The rFnbA was incubated in the presence of factor XIIIa and a molar excess of fluorescent probe. At various times, aliquots of reaction mixtures with dansylcadaverine or dansyl-ϵ-aminocaproyl-QQIV were collected, analyzed by SDS−PAGE, and examined under ultraviolet light prior to staining with Coomassie Blue (Figure 6). From the photographs taken under ultraviolet illumination, it is apparent that factor XIIIa catalyzed the incorporation of both probes into rFnbA in a time-dependent manner. In the presence of 2 mM dansylcadaverine, the band corresponding to rFnbA undergoes a continual increase of fluorescence reflecting the attachment of increasing molecules of probe (Figure 6A). Under the same experimental conditions, other

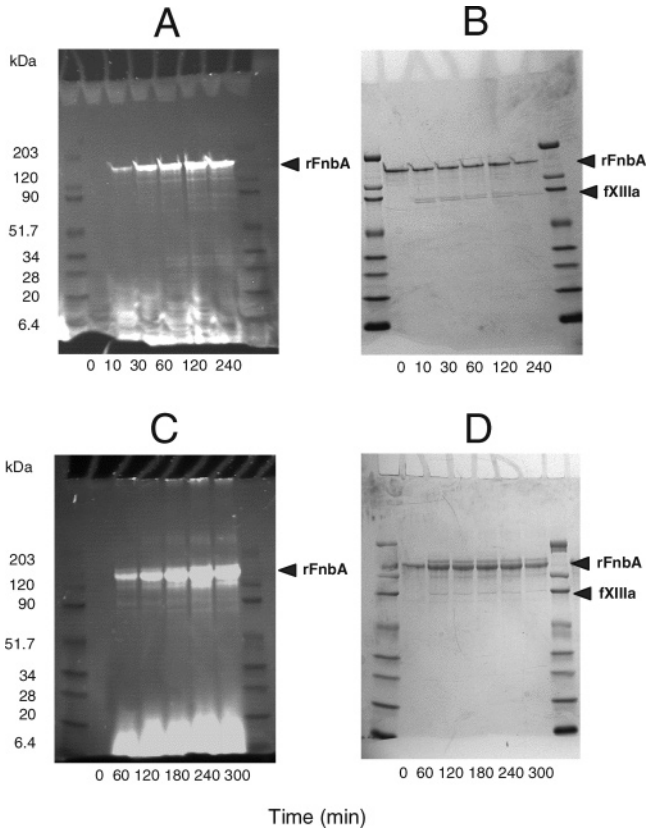

FIGURE 6: Factor XIIIa-catalyzed incorporation of dansylcadaverine (A and B) and dansyl-ϵ-aminocaproyl-QQIV (C and D) into rFnbA. The rFnbA (2 μM) was reacted with thrombin-activated factor XIIIa (30 μg/mL) in the presence of the molar excess of the glutamine-labeling probe dansylcadaverine (2 mM) or the lysine decorating peptide dansyl-ϵ-aminocaproyl-QQIV (2 mM) in TBS, pH 7.4, 5 mM DTT, 5 mM $CaCl_2$ buffer at 37 °C. Aliquots were removed at the indicated time points, mixed with SDS under reducing conditions, heated, and analyzed by SDS−PAGE on 4−20% gradient gels. After electrophoresis, the gels were photographed under ultraviolet light (A and C) and then stained with Coomassie Brilliant Blue (B and D). The brightly fluorescent material at the bottom of the gels photographed under ultraviolet light is unreacted dansylcadaverine and dansyl-ϵ-aminocaproyl-QQIV peptide. Arrows show positions of rFnbA and factor XIIIa. The outer lanes in the gels contain molecular mass standards as indicated.

tested proteins, including bovine serum albumin and recombinant fragments of fibrinogen-binding protein from *S. aureus* (ClfA) and from *S. epidermidis* (SdrG) failed to incorporate dansylcadaverine (not shown). A gradual increase of fluorescence intensity of the rFnbA band also was clearly visible when the reaction was carried out in the presence of 2 mM dansyl-ϵ-aminocaproyl-QQIV (Figure 6C). When rFnbA was incubated alone with factor XIIIa, the band on the SDS−PAGE corresponding to monomeric protein became depleted. This process was accompanied by the appearance of high molecular mass polymers that failed to enter the gel (not shown). Collectively, these results clearly indicate that the fibronectin binding protein carries reactive Gln and Lys residues and therefore acts as a bifunctional substrate for factor XIIIa.

Factor XIIIa-Catalyzed Covalent Cross-Linking of Fibronectin-Binding Protein to Fibronectin. To test whether a reversible complex between Staphylococcal fibronectin-binding protein and fibronectin could be covalently stabilized by the transglutaminase action of factor XIIIa, we performed

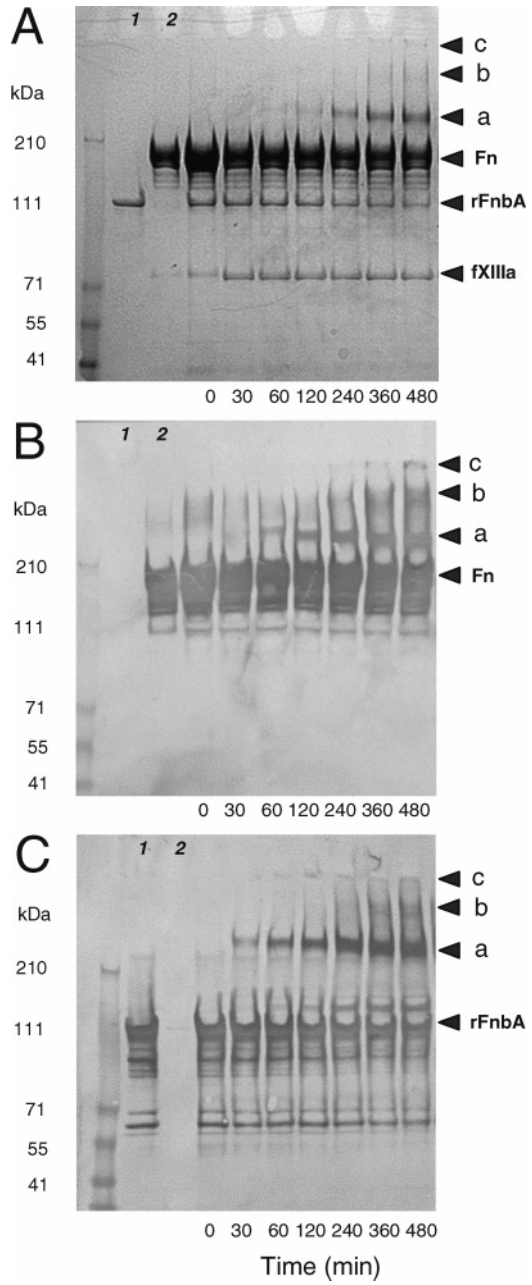

FIGURE 7: Factor XIIIa-catalyzed cross-linking between rFnbA and fibronectin. The rFnbA (1 μM) was incubated in the presence of fibronectin (2 μM) and factor XIIIa (15 μg/mL) in TBS, pH 7.4, 5 mM $CaCl_2$ buffer at 25 °C. Aliquots were removed at the indicated time points, mixed with SDS under reducing conditions, heated, and analyzed by SDS−PAGE on 4−20% gradient gels. After electrophoresis, the gels were either stained with Coomassie Brilliant Blue (A) or subjected to transfer to nitrocellulose filters followed by immunostaining with anti-fibronectin (B) and anti-rFnbA (C) antibodies. Lanes 1 and 2 in each panel contain the rFnbA and fibronectin, respectively. Arrows show positions of the rFnbA, fibronectin, factor XIIIa, and products of cross-linking reaction depicted as a, b, and c. The left-hand lane in each panel contains molecular mass standards as indicated.

cross-linking reactions and analyzed thereby the SDS−PAGE and Western blot assays. Upon incubation of fibronectin-binding protein in the presence of fibronectin and factor XIIIa, the band corresponding to rFnbA was steadily depleted as both proteins became cross-linked into high-molecular mass species (Figure 7 A). Formation of covalently cross-linked heteropolymers consisting of fibronectin-binding

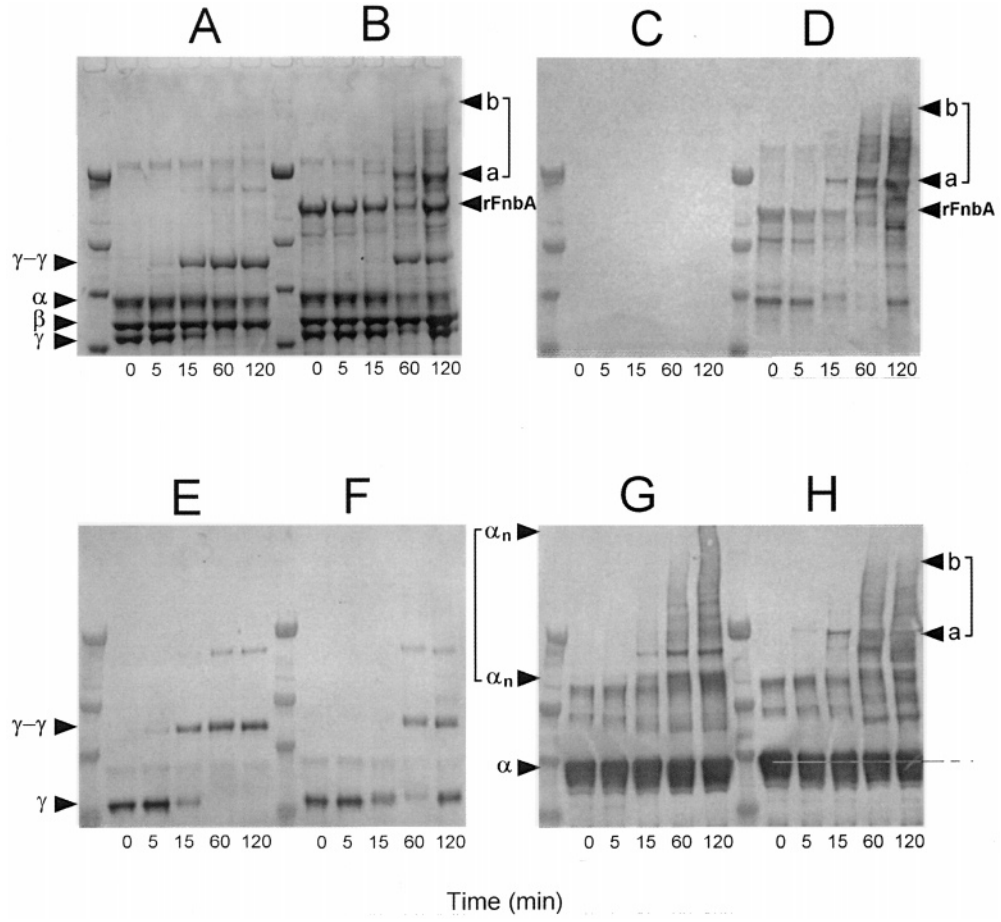

FIGURE 8: Factor XIIIa-catalyzed cross-linking of rFnbA to fibrin. Cross-linking was initiated by the addition of thrombin (0.5 U/mL) at time zero to 5 μM fibrinogen and 15 μg/mL factor XIII in the absence (A, C, E, and G) and presence (B, D, F, and H) of 2 μM rFnbA. Reactions were performed in TBS, pH 7.4, 5 mM $CaCl_2$ buffer at 25 °C. At indicated time points, cross-linking reactions were terminated and analyzed by SDS−PAGE on 3−8% gradient gels under reducing conditions. After electrophoresis, the gels were either stained with Coomassie Brilliant Blue (A and B) or subjected to transfer to nitrocellulose filters followed by immunostaining with anti-rFnbA (C and D), anti-fibrinogen γ chain (E and F), and anti-fibrinogen α chain (G and H) antibodies. Arrows show positions of rFnbA and the α, β, and γ chains of fibrin. The products of fibrin cross-linking are indicated as $\gamma\gamma$ dimers and various size α_n polymers, while the products of cross-linking between rFnbA and fibrin are depicted as a spectrum of low mobility bands ranging from a to b. The left-hand lane in each panel contains molecular mass standards having, from top to bottom, the following M_r values: 210, 125, 101, and 56.2 kDa.

protein and fibronectin was evident from results of Western blot analyses using anti-fibronectin monoclonal antibody (Figure 7B) and anti-rFnbA polyclonal antibody (Figure 7C). As shown in Figure 7B,C, both antibodies reacted with the newly formed low mobility bands a, b, and c, strongly suggesting that factor XIIIa catalyzes covalent cross-linking between Staphylococcal fibronectin-binding protein and human fibronectin.

Factor XIIIa-Catalyzed Covalent Cross-Linking of Fibronectin-Binding Protein to Fibrin. The effect of Staphylococcal fibronectin-binding protein on factor XIIIa-catalyzed fibrin cross-linking was investigated by SDS−PAGE and Western blot analysis. As shown in Figure 8A, in the control reaction at time zero under reducing conditions, fibrin migrates as three bands corresponding to α, β, and γ chains. Cross-linking of fibrin by factor XIIIa resulted in rapid disappearance of the γ chain, which was accompanied by formation of $\gamma\gamma$ dimers (Figure 8A,E). Depletion of the fibrin α chain band and formation of the α chain cross-linked polymers occurred at a much slower rate and was not easily detectable on SDS−PAGE (Figure 8A) but was clearly visible upon immunostaining of the blot with anti-fibrinogen α chain monoclonal antibody (Figure 8G). When fibronectin-binding protein was included in the reaction mixture, it led to several obvious changes in the fibrin cross-linking pattern. Upon incubation of fibrin with factor XIIIa, the band corresponding to the rFnbA was progressively depleted, while multiple new high molecular mass bands appeared on SDS−PAGE (Figure 8B, bands a and b). These new bands cross-reacted with both anti-rFnbA polyclonal antibody (Figure 8D) and anti-fibrinogen α chain monoclonal antibody (Figure 8H) but did not react with anti-fibrinogen γ chain monoclonal antibody (Figure 8F). These data suggest that the new high molecular mass bands detected by SDS−PAGE and Western blot analysis represent heterocomplexes composed of fibronectin-binding protein covalently cross-linked to the fibrin α chains. The apparent molecular mass of these cross-linked complexes is consistent with the formation of α chain polymers to which one or more fibronectin-binding proteins are attached. The presence of fibronectin-binding protein in the reaction mixture also affected the rate of $\gamma-\gamma$ chain cross-linking (Figure 8E,F). At tested conditions, the formation of $\gamma\gamma$ dimers was delayed (Figure 8F), suggesting that fibronectin-binding protein inhibits this process.

DISCUSSION

The results presented here indicate that full-length recombinant FnbA (Ala1 to Pro839) and fluorescein-labeled rFnbA interact with immobilized fibronectin with K_d values of 0.12 and 0.79 nM, respectively (Figure 2). The apparent affinity of this interaction is comparable to that reported for the binding of *S. aureus* cells to fibronectin and its NH_2-terminal 29 kDa Fib-1 fragment (*28*, *29*) (K_d = 1.8−5.6 nM) or for binding of the rD1-3 fragment of fibronectin-binding protein to 29 kDa Fib-1 fibronectin fragment (*30*) (K_d = 1.5 nM). The strong interaction between these two proteins with K_d values in the subnanomolar/low nanomolar range was employed in this study to address the question of the stoichiometry of association. Analytical size-exclusion chromatography revealed that full-length rFnbA accommodates at least two molecules of fibronectin. Because of restrictions of the method employed, the association of more than two molecules of fibronectin with FITC-rFnbA could not be detected, and therefore, the existence of additional fibronectin-binding sites within FnbA is quite possible. The Staphylococcal-binding site of fibronectin is located within the NH_2-terminal Fib-1 region, which is composed of five type-I or finger domains (*31*). The major site responsible for binding with FnbA was further delimited to the region consisting of the two finger domains, four and five (*30*). Interestingly, the NH_2-terminal fibrin-binding site of fibronectin is also formed by the same fourth and fifth finger domains (*16*), indicating that binding to FnbA may prevent the incorporation of fibronectin into fibrin clot. Earlier studies demonstrated that the stoichiometry of association between the NH_2-terminal 29 kDa Fib-1 fragment of fibronectin and the COOH-terminal D1-D3 repeat fragment of fibronectin-binding protein is equal to 1.9:1 (*30*). Since fibronectin is composed of two chains, the results of our size-exclusion chromatography experiments imply that in the presence of two molar excess of fibronectin, each FnbA associates with two NH_2-terminal regions representing two different fibronectin molecules, while the second pair of their NH_2-terminal sites remains unoccupied. This might be caused by the inability of the NH_2-terminus of the free chain of fibronectin dimer to engage the second complementary site on the Staphylococcal receptor due to flexibility constraints. Alternative scenarios, however, cannot be excluded, especially if the COOH-terminal Fib-2 region of fibronectin (*32*) indeed participates in receptor−ligand binding.

When factor XIIIa is present in the reaction mixture, the reversible complex between fibronectin-binding protein and fibronectin is covalently stabilized by the introduction of intermolecular isopeptide bond(s). The identity of high molecular mass products of the cross-linking reaction detected on SDS−PAGE was demonstrated by Western blot analysis. These high molecular mass bands were cross-reactive with both anti-fibronectin monoclonal and anti-rFnbA polyclonal antibodies, strongly suggesting their heteropolymeric origin (Figure 8). It is well-established that fibronectin serves as a monofunctional substrate for factor XIIIa that contains a reactive glutamine residue located in the third position within its NH_2-terminal region (*33*). Therefore, factor XIIIa most likely catalyzes the formation of the ϵ-(γ-glutamyl)lysine isopeptide bond between NH_2-terminal reactive glutamine residue of fibronectin and reactive lysine residue(s) of FnbA. This speculation is supported by an earlier report that fibronectin and its NH_2-terminal Fib-1 region undergoes factor XIIIa-catalyzed cross-linking to the surface of *S. aureus* (*31*). It seems very likely that Staphylococcal FnbA is directly involved in this cross-linking reaction resulting in the covalent attachment of fibronectin to the surface of the microorganism.

Binding of rFnbA to immobilized fibrinogen and fibrin occurs with high affinity with K_ds of 30.2 and 29.3 nM, respectively (Figure 4). These data indicate that Staphylococcal FnbA may bind equally well either to soluble fibrinogen circulating in plasma or to the fibrin clot formed at the site of vascular injury. Treatment of fibrinogen with thrombin utilized in this study for the generation of fibrin, however, may result in the formation of immobilized fibrin monomer instead of fibrin protofibrils. This scenario assumes that the FnbA-binding site(s) may not be readily available in the polymeric fibrin. Even though, in the case of fibronectin-fibrin(ogen) interaction, it was demonstrated that fibrinogen immobilized on a plastic and treated with thrombin behaves as polymeric fibrin (*15*), the possibility that the employed procedure produced immobilized fibrin monomer cannot be excluded. According to earlier published data, the FnbA-binding site is localized in the 17 residues COOH-terminal region of the fibrinogen γ chain (*4*). The reported K_d value of the FnbA−fibrinogen interaction estimated in this study by the surface plasmon resonance (SPR) technique was, however, much higher (11 μM) (*4*) than that determined here using an ELISA-based assay. Such a discrepancy might be caused by partial destruction and/or obscuring of the binding site(s) during covalent immobilization of fibrinogen to the sensor chip (*4*). Apparently, this does not take place upon immobilization to the plastic of microplate wells. To characterize further the interaction between rFnbA and fibrin(ogen), we have investigated the effect of rFnbA on thrombin-induced fibrin polymerization using a turbidometric method. Incorporation of increasing concentrations of rFnbA into the reaction mixture containing 1 μM fibrin causes a lower turbidity, longer lag period, and slower maximum rate of turbidity increase as compared to the control (Figure 5). The maximum effect resulting in complete inhibition of fibrin assembly was observed in the presence of 0.5 μM rFnbA (Figure 5), which translates into a molar ratio of one rFnbA to two fibrin molecules. This result is consistent with the role of the COOH-terminal region of fibrin(ogen) γ chain in both binding of FnbA (*4*) and fibrin polymerization (*34*, *35*). Binding of rFnbA to the COOH-terminus of fibrin(ogen) γ chain results in occupation and/or steric hindrance of the major polymerization site and subsequent inhibition of the protofibril assembly. Another evidence supporting this interpretation is provided by the effect of rFnbA on the lag phase of the fibrin polymerization curves. When the concentration of FnbA in the reaction mixture was increased from 0 to 0.2 μM, the time of lag phase extended from 300 to 600 s (Figure 5), again strongly suggesting inhibition of the protofibril formation stage.

The results of the fibrin polymerization light scattering experiments are in good agreement with the factor XIIIa-catalyzed fibrin cross-linking data. Incorporation of rFnbA in the factor XIIIa-catalyzed fibrin cross-linking reaction resulted in partial inhibition of $\gamma-\gamma$ cross-links (Figure 8B,F) and in the covalent incorporation of rFnbA into α chain

polymers (Figure 8B,H). The $\gamma-\gamma$ cross-linking between two end-to-end oriented fibrin molecules takes place via reactive Lys 406 and Gln 398 residues situated close to the carboxy-terminus of the γ chain (*36*). The same Lys 406 and Gln 398 residues also participate in formation of the FnbA-binding site that was narrowed down to the final 17 residues at the COOH-terminal end of the γ chain (*4*). Association of FnbA with fibrin competes with factor XIIIa-catalyzed $\gamma-\gamma$ cross-linking resulting in the delay of $\gamma-\gamma$ dimer formation as compared to the control reaction (Figure 8). Reversible binding of FnbA to the COOH-terminus of the γ chain is stabilized by factor XIIIa, which covalently attaches FnbA to the fibrin α chains (Figure 8). Unlike γ chains, which form closed reciprocally cross-linked dimers, α chains become cross-linked into extensive multimeric arrays due to the presence of multiple glutaminyl acceptors and lysine donor sites (*23*, *37*, *38*). Cross-linking of FnbA to the α chains of fibrin, therefore, may occur via its reactive glutamine(s), lysine(s), or a combination of both.

The data presented in this study clearly demonstrate that Staphylococcal rFnbA serves as a bifunctional substrate for factor XIIIa. Evidence for this has been obtained using a primary amine dansylcadaverine that labels reactive glutamine-(s) as well as a dansylated peptide patterned on the N-terminal sequence of fibronectin that labels reactive lysine-(s) (Figure 6). In addition, in the presence of active factor XIII, FnbA forms large molecular homopolymers that failed to enter the gel upon SDS−PAGE analysis, again suggesting the presence within FnbA of both reactive glutamines and lysines. The existence of reactive glutamine and lysine residues within FnbA indicates that they must be involved in factor XIIIa catalyzed cross-linking between FnbA and its ligands. Because of their physiological importance and well-established affinity to FnbA, we have proposed that both fibronectin and fibrin(ogen) are suitable cross-linking partners for Staphylococcal FnbA. Our data demonstrate the formation of high molecular mass cross-linked heteropolymers when FnbA is incubated in the presence of factor XIIIa and fibronectin (Figure 7) or fibrin (Figure 8). Both fibronectin and fibrin(ogen) serve as major substrates for plasma and tissue transglutaminases and undergo cross-linking reactions with each other as well as other proteins (*21*). Furthermore, plasma transglutaminase circulates in blood mostly in association with fibrinogen (*39*), while tissue transglutaminase is known to form tight complexes with fibronectin (*40*, *41*). Thus, reversible binding of Staphylococcal FnbA to either of its ligands would result in the formation of the ternary complex between transglutaminase and its substrates required for the initiation of a cross-linking reaction. Such covalent cross-linking might be critical for stabilization of initial bacterial adherence, which plays a central role in host-to-host transmission and the maintenance of stable carriage of *S. aureus*. Factor XIIIa-catalyzed cross-linking of *S. aureus* to fibronectin and fibrin might play an especially important role upon microbial colonization at the site of vascular injury. By incorporation into the wound site, FnbA has the capacity to inhibit fibrin polymerization and wound healing reactions. Followed by initial colonization at the site of the injury, these activities of the FnbA subsequently could play an important role in promoting the dissemination of infection. Ability of FnbA to undergo cross-linking to fibronectin and fibrin may also contribute to adherence of *S. aureus* to tissues and implanted medical devices. Further evaluation of factor XIIIa-catalyzed Staphylococcal cross-linking to fibronectin and fibrin(ogen) requires identification of reactive glutamine acceptor and lysine donor site(s) within FnbA. These experiments are currently under way in our laboratory.

ACKNOWLEDGMENT

We thank Dr. Leah Fletcher for her help with DNA sequencing of the cloned *fnb*A gene and Michael G. Wetherell for assistance with protein sequence analysis. We also thank Dr. Stephen A. Udem for critical reading of the manuscript.

REFERENCES

1. Patti, J. M., Allen, B. L., McGavin, M. J., and Hook, M. (1994) *Annu. Rev. Microbiol. 48*, 585−617.
2. Froman, G., Switalski, L. M., Speziale, P., and Hook, M. (1987) *J. Biol. Chem. 262*, 6564−6571.
3. Flock, J. I., Froman, G., Jonsson, K., Guss, B., Signas, C., Nilsson, B., Raucci, G., Hook, M., Wadstrom, T., and Lindberg, M. (1987) *EMBO J. 8*, 2351−2357.
4. Wann, E. R., Gurusiddappa, S., and Hook, M. (2000) *J. Biol. Chem. 275*, 13863−13871.
5. Joh, H. J., House-Pompeo, K., Patti, J. M., Gurusiddappa, S., and Hook, M. (1994) *Biochemistry 33*, 6086−6092.
6. Signas, C., Raucci, G., Jonsson, K., Lindgren, P. A., Anantharamaiah, G. M., Hook, M., and Lindberg, M. (1989) *Proc. Natl. Acad. Sci. U.S.A. 86*, 699−703.
7. Jonsson, K., Signas, C., Muller, H. P., and Lindberg, M. (1991) *Eur. J. Biochem. 202*, 1041−1048.
8. Joh, D., Speziale, P., Gurusiddappa, S., Manor, J., and Hook, M. (1998) *Eur. J. Biochem. 258*, 897−905.
9. Schneewind, O., Fowler, A., and Faull, K. F. (1995) *Science 268*, 103−106.
10. Doolittle, R. F. (1987) in *Haemostasis and Thrombosis* (Bloom, A. L., and Thomas, D. P., Eds.) pp 192−215, Churchill Livingstone, Edinburgh.
11. Hynes, R. O. (1990) *Fibronectins*, Springer-Verlag, New York.
12. Henschen, A., and McDonagh, J. (1986) in *Blood coagulation* (Zwaal, R. F. A., and Hemker, H. C., Eds.) pp 171−241, Elsevier Science Publishers, Amsterdam.
13. Mosher, D. F., and Johnson, R. B. (1983) *Ann. N.Y. Acad. Sci. 408*, 583−593.
14. Sekiguchi, K., and Hakomori, S. (1983) *J. Biol. Chem. 258*, 3967−3973.
15. Makogonenko, E., Tsurupa, G., Ingham, K., and Medved, L. (2002) *Biochemistry 41*, 7907−7913.
16. Matsuka, Y. V., Medved, L. V., Brew, S. A., and Ingham, K. C. (1994) *J. Biol. Chem. 269*, 9539−9546.
17. Matsuka, Y. V., Migliorini, M., and Ingham, K. C. (1997) *J. Protein Chem. 16*, 739−745.
18. Grinnel, F., Feld, M., and Minter, D. (1980) *Cell 19*, 517−525.
19. Knox, P., Crooks, S., and Rimmer, C. S. (1986) *J. Cell Biol. 102*, 2318−2323.
20. Corbett, S. A., Lee, L., Wilson, C. L., and Schwarzbauer, J. E. (1997) *J. Biol. Chem. 272*, 24999−25005.
21. Lorand, L. (2001) *Ann. N.Y. Acad. Sci. 936*, 291−311.
22. Ingham, K., and Brew, S. (1981) *Biochim. Biophys. Acta 670*, 181−189.
23. Parameswaran, K. N., Velasco, P. T., Wison, J., and Lorand, L. (1990) *Proc. Natl. Acad. Sci. U.S.A. 87*, 8472−8475.
24. Lorand, L., Velasco, P. T., Murthy, S. N. P., Wison, J., and Parameswaran, K. N. (1992) *Proc. Natl. Acad. Sci. U.S.A. 89*, 11161−11163.
25. Lorand, L., Parameswaran, K. N., Velasco, P. T., and Murthy, S. N. P. (1992) *Bioconjugate Chem. 3*, 37−41.
26. Hantgan, R. R., and Hermans, J. (1979) *J. Biol. Chem. 254*, 11272−11281.
27. Hantgan, R. R., Fowler, W., Erickson, H., and Hermans, J. (1980) *Thromb. Haemostasis 44*, 119−124.
28. Proctor, R. A., Mosher, D. F., and Olbrantz, P. J. (1982) *J. Biol. Chem. 257*, 14788−14794.

29. Bozzini, S., Visai, L., Pignatti, P., Petersen, T. E., and Speziale, P. (1992) *Eur. J. Biochem. 207*, 327−333.
30. Huff, S., Matsuka, Y. V., McGavin, M. J., and Ingham, K. C. (1994) *J. Biol. Chem. 269*, 15563−15570.
31. Mosher, D. F., and Proctor, R. A. (1980) *Science 209*, 927−929.
32. Sakata, N., Jakab, E., and Wadstrom, W. (1994) *J. Biochem. 115*, 843−848.
33. McDonagh, R. P., McDonagh, J., Peterson, T. E., Thorgersen, H. S., Skorstengaard, K., Sottrup-Jensen, L., and Magnusson, S. (1981) *FEBS Lett. 127*, 174−178.
34. Shimizu, A., Nagel, G. M., and Doolittle R. F. (1992) *Proc. Natl. Acad. Sci. U.S.A. 89*, 2888−2892.
35. Medved, L., Litvinovich, S., Ugarova, T., Matsuka, Y., and Ingham, K. (1997) *Biochemistry 36*, 4685−4693.
36. Chen, R., and Doolittle, R. F. (1971) *Biochemistry 10*, 4486−4491.
37. Cottrell, B. A., Strong, D. D., Watt, K. W. K., and Doolittle, R. F. (1979) *Biochemistry 18*, 5405−5410.
38. Matsuka, Y. V., Medved, L. V., Migliorini, M. M., and Ingham, K. C. (1996) *Biochemistry 35*, 5810−5816.
39. Greenberg, C. S., and Shuman, M. A. (1982) *J. Biol. Chem. 257*, 6096−6101.
40. Lorand, L., Dailey, J. E., and Turner, P. M. (1988) *Proc. Natl. Acad. Sci. U.S.A. 85*, 1057−1059.
41. LeMosy, E. K., Erickson, H. P., Beyer, W. F., Radek, J. T., Jeong, J.-M., Murthy, S. N. P., and Lorand, L. (1992) *J. Biol. Chem. 267*, 7880−7885.

BI035239H